Neoplasma 2023; 70(4): 566–579

doi:10.4149/neo_2023_230410N196

miRNA-329-3p suppresses proliferation and metastasis of endometrial carcinoma through downregulating *E2F1*

Ruicong WANG, Chen ZHANG, Wanting GUAN, Qing YANG*

Department of Obstetrics and Gynecology, Shengjing Hospital of China Medical University, Shenyang, Liaoning, China

**Correspondence: Yangqing_sj@126.com*

Received April 10, 2023 / Accepted August 25, 2023

Existing evidences have revealed the crucial roles of E2 promoter binding factor-1 (*E2F1*) during the tumorigenesis and progression process of multiple human tumors. However, the expression patterns, biological functions, as well as the underlying molecular mechanism of *E2F1* in endometrial carcinoma yet remain largely unclear. The expression patterns and clinical prognostic value of *E2F1* in endometrial carcinoma were evaluated using bioinformatics methods. Protein and mRNA, miRNA expression levels in tissues and cells were measured using immunohistochemistry, western blotting, and qRT-PCR assays. Cell viability and cell cycle distribution were examined using CCK-8 assay and flow cytometry, respectively. Scratch healing assay and Transwell assay were applied to measure cell migration and invasion ability. Bioinformatic analysis and luciferase reporter assays were conducted to confirm the targeting relationship between *E2F1* and miR-329-3p. Moreover, a series of *in vitro* and *in vivo* functional experiments were employed to evaluate the effect of the miR-329-3p/*E2F1* axis on cell growth and metastasis. Clinically, *E2F1* was aberrantly expressed in endometrial carcinoma tissues and was correlated with advanced FIGO stage, histological type, p53 mutation, poor survival, and degree of tumor cell differentiation. ROC curves analysis also reveals that *E2F1* has a high AUC value (up to 0.952, 95% CI: 0.915-0.988), indicating the promising diagnostic value of *E2F1* level in endometrial carcinoma. In addition, *in vitro* gain and loss-of-functional experiments verified that high *E2F1* can promote cell proliferation, cell cycle, migration, invasion, and EMT process. In-depth mechanism studies revealed that *E2F1* was a downstream target gene of miR-329-3p, and miR-329-3p overexpression could effectively abrogate its promotion of cell malignant biological behavior. Collectively, our findings suggested that the miR-329-3p/*E2F1* axis plays a crucial role in the progression of endometrial carcinoma, indicating that *E2F1* can be considered a promising diagnostic and prognostic biomarker for endometrial carcinoma patients.

Key words: endometrial carcinoma; E2F1, miR-329-3p; metastasis; EMT

Endometrial cancer (EC) is the most common gynecologic malignancy, typically occurring between the ages of 65 and 75, particularly in perimenopausal and postmenopausal women [1]. The incidence and mortality rates of EC have been on the rise in recent years due to the increasing prevalence of obesity, mental stress, and poor dietary habits. Despite advancements in early cancer screening, patients with advanced stage disease (stage III: 47–58%, stage IV: 15–17%) continue to experience poorer 5-year survival rates [2–4]. Therefore, there is an urgent need to explore the underlying pathological mechanisms and discover potential biomarkers for the diagnosis, treatment, and prognosis of EC.

E2 promoter binding factors (E2Fs) belong to an important transcription factor family that regulates gene expression involved in cell cycle, apoptosis, senescence, and metastasis [5–7]. To date, eight members of this family (*E2F1-8*) have been identified in the human genome. Among them, *E2F1* is the most extensively studied and plays a crucial role in tumorigenesis [8]. Initially classified as an oncogene, *E2F1* has been found to be aberrantly expressed and positively associated with poor prognosis in various solid tumors, including lung cancer [9], prostate cancer [10], breast cancer [11], colorectal cancer [12], and gastric cancer [13]. Interestingly, recent studies have provided evidence suggesting that *E2F1* can also act as a tumor suppressor depending on the cellular context, indicating a complex role of *E2F1* in cancer development and progression [14]. Although several studies have demonstrated aberrant expression of *E2F1* in EC and its predictive value for the prognosis of EC patients [15–17], the specific expression patterns, biological functions, and

underlying mechanisms of *E2F1* in the context of EC remain largely elusive. Therefore, further investigation into the role of *E2F1* in EC may offer a promising target and biomarker for EC patients.

MicroRNAs (miRNAs) are a subclass of non-coding RNA molecules, approximately 22 nucleotides in length, that play pivotal roles in physiological and pathological processes by binding to the 3'untranslated region (3'-UTR) of complementary target genes, leading to translational inhibition or degradation [18–20]. Recently, increasing evidence has confirmed the dominant roles of miRNAs in development, diseases, particularly cancer, and they are considered attractive tools and targets for the diagnosis and treatment of malignant tumors [21]. Notably, several miRNA-targeted therapeutics, such as miRNA-34 mimics, have shown promising effectiveness in pre-clinical and phase I–II clinical trials [22]. Emerging evidence suggests that miR-329-3p is involved in the carcinogenesis and progression of various tumors (cervical cancer, hepatocellular carcinoma, and neuroblastoma) by acting as a tumor suppressor and regulating multiple cellular processes, including cell proliferation, apoptosis, metastasis, chemoresistance, and stemness [23–25]. However, the biological functions and molecular mechanisms of miR-329-3p in EC are not fully understood and require further elucidation.

In this study, bioinformatics analysis of TCGA database revealed aberrant expression of *E2F1* in EC tissues, positively correlated with poor outcomes, suggesting an oncogenic role in EC development and progression. Furthermore, considering the tumor suppressor role of miR-329-3p and predictions from miRDB (http://mirdb.org/cgi-bin/search.cgi) and Target Scan (http://www.targetscan.org/), it was hypothesized that miR-329-3p might attenuate EC progression by targeting *E2F1*. This hypothesis was validated through *in vitro* and *in vivo* experiments. As anticipated, the results demonstrated that *E2F1* promotes cell proliferation, cell cycle progression, and metastasis, while miR-329-3p directly binds to the 3'-UTR of *E2F1*, thereby counteracting these effects.

Patients and methods

Clinical tissue specimens. A total of 17 human simple hyperplasia tissues, 22 human atypical hyperplasia tissues, and 40 human EC tissues were collected from patients who underwent surgical resection at Shengjing Hospital of China Medical University from July 2018 to February 2022. Immediately after excision, all specimens were snap-frozen in liquid nitrogen for subsequent immunohistochemical analysis or RNA isolation. The study protocol was approved by the Ethics Committee of Shengjing Hospital of China Medical University (Permission number: 2021PS723K), and written informed consent was obtained from all patients.

Cell culture. Three different human EC cell lines with varying degrees of differentiation (Ishikawa, HEC-1A, and KLE) were obtained from ATCC, and their identities were confirmed through STR profiling. Ishikawa cells were cultured in the RPMI-1640 medium, HEC-1A cells in the McCoy's 5A medium, and KLE cells in the DMEM/F12 medium. All culture media were supplemented with 10% fetal bovine serum and 1% penicillin/streptomycin. The cells were maintained in a humidified incubator at 37 °C with 5% CO_2.

Immunohistochemistry (IHC). Immunohistochemical (IHC) analysis for *E2F1* in human tissues was conducted following a previously described standard protocol. Tissue sections with a thickness of 5 μm were incubated overnight at 4 °C with a primary antibody against *E2F1* (1:100). Subsequently, the sections were incubated with IgG(H+L) (HRP-labeled Goat Anti-Mouse IgG (H+L)) (1:500) for 1 hour at 37 °C. Hematoxylin staining was used to counterstain the cell nuclei, and the Olympus multifunction microscope was utilized to observe the *E2F1*-positive area. The immunohistochemical scoring was calculated based on a previously established protocol.

qRT-PCR analysis. Total RNA was extracted from tissues or cell lines using a TRIzol reagent. For qRT-PCR analysis, reverse transcription was performed using a Reverse Transcription Kit according to the standard protocol. β-actin was chosen as the internal control to normalize gene expression. Details of the primers are provided in Table 1.

Western blot analysis. After administering the desired treatment, cells were collected and lysed with RIPA buffer containing PMSF protease inhibitor (1:100). The isolated protein samples were quantified using a BCA kit following the manufacturer's instructions. Subsequently, the protein samples were subjected to polyacrylamide gel electrophoresis, following a procedure described in a previous study. Primary antibodies against *E2F1* (1:1000, #WL02394), E-cadherin (1:1000, #WL01482), Vimentin (1:1000, #WL00742), and β-actin (1:1000, #WL01372) were purchased from Wanleibio (Shanghai, China). Finally, the blot images were visualized

Table 1. The primer sequence information for qRT-PCR.

Primer name	Primer sequence (5'-3')
E2F1 (Forward)	ACTCCTCGCAGATCGTCA
E2F1 (Reverse)	TCCAGCCTCCGCTTCAC
E-cadherin (Forward)	GAACGCATTGCCACATACAC
E-cadherin (Reverse)	GCACCTTCCATGACAGACCC
Vimentin (Forward)	CCTTGACATTGAGATTGCCACCTA
Vimentin (Reverse)	TCATCGTGATGCTGAGAAGTTTCG
MMP2 (Forward)	TGGCAAGGAGTACAACAGC
MMP2 (Reverse)	TGGAAGCGGAATGGAAAC
MMP9 (Forward)	AGGACGGCAATGCTGATG
MMP9 (Reverse)	TCGTAGTTGGCGGTGGTG
β-actin (Forward)	GGCACCCAGCACAATGAA
β-actin (Reverse)	TAGAAGCATTTGCGGTGG

using an enhanced ECL kit and processed using ImageJ software.

Cell viability assessment. Cells at the logarithmic growth phase were seeded at a density of 4,000 cells/well in 96-well plates. After the desired incubation time, 10 μl of CCK-8 working solution was added to each well, and the cells were further incubated for 2 h until the solution turned yellow-orange in color. Subsequently, the absorbance at 450 nm was measured using a multifunctional microplate reader.

Cell cycle analysis. Cells were seeded into 6-well plates at a concentration of 3×10^5 cells/well and incubated for an additional 24 h. After the desired treatment, the cells were harvested and fixed with 1 ml of 70% cold ethanol at 4 °C overnight. Subsequently, the cells were washed three times with PBS and incubated with 100 μl of RNase A at a 37 °C water bath for 30 min. Following this, the cells were stained with 500 μl of propidium iodide for 30 min at 4 °C in the dark. Finally, the cell cycle distribution was examined using flow cytometry and FlowJo software v10 (FlowJo, LLC) was utilized for cell cycle analysis.

Wound scratch assay. Cells were seeded into 6-well plates at a concentration of 5×10^5 cells/well and cultured until reaching approximately 95–100% confluence. Subsequently, a scratch was created on the cell monolayer using a sterile 20 μl pipette tip, and the wells were washed three times with PBS to remove any detached cells. The scratch wounds were then observed and captured using an inverted Olympus IX70 microscope at 0 h and 24 h. The scratch healing rate was calculated using ImageJ software according to the following formula: Wound healing rate (%) = (0-hour scratch area – 24-hour scratch area)/0-hour scratch area × 100%.

Transwell assay. A total of 5×10^3 cells were suspended in 200 μl of a serum-free medium and added to the upper chamber of a Transwell insert. Matrigel was used to coat the insert for the cell invasion assay, while for the cell migration assay, the insert was left uncoated. Subsequently, 800 μl of fresh medium containing 10% FBS was added to the lower chamber, and the cells were cultured for an additional 24 h. After the incubation period, any non-invasive or non-migratory cells remaining in the upper chamber were gently swabbed off using a cotton swab. Meanwhile, the cells on the bottom side of the Transwell chamber were fixed with 4% polyformaldehyde for 20 min at room temperature and then stained with 0.1% crystal violet for 5 min. Following three washes with deionized water, the invasive or migratory cells were observed and photographed under a microscope at 200× magnification.

Cell transfection. To reduce *E2F1* expression in KLE cells, General Biology (Anhui, China) synthesized three *E2F1*-targeted siRNA sequences (siRNA 1, siRNA 2, and siRNA 3) along with a siRNA-NC. After transfection for 48 h, we confirmed the transfection efficiency of these *E2F1* siRNAs by detecting the mRNA and protein levels of *E2F1*. Subsequently, we selected the most effective *E2F1* siRNA for further experiments.

For the overexpression of *E2F1* in Ishikawa cells, we subcloned a human *E2F1* overexpression vector (pcDNA3.1-*E2F1*) and an empty plasmid pcDNA3.1 into a lentivirus vector. Furthermore, we obtained hsa-miR-329-3p mimics, inhibitor, and negative control from GenePharma (Shanghai, China), and transfected them into cells using Lipofectamine 3000 following the manufacturer's standard protocols.

Dual-luciferase reporter assay. GenePharma (Shanghai, China) designed and synthesized the sequences of hsa-miR-329-3p mimics or *E2F1* 3'UTR, which included both the wild-type (wt) and mutant (Mut) binding sites of hsa-miR-329-3p. Subsequently, co-transfection of hsa-miR-637 mimics/miR-NC and *E2F1*-wt/Mut plasmids was performed in 293T cells using Lipofectamine 3000. After a 48 h transfection period, the activities of firefly and Renilla luciferase were determined using the Dual Luciferase Reporter Assay Kit, following the manufacturer's instructions.

Animal experiments. 4–5-week-old male BALB/c nude mice were obtained from Shanghai Laboratory Animal Company (SLAC, Shanghai, China) and housed in a specific pathogen-free environment. All animal experiments were conducted in accordance with the Animal Care and Use Committee of Shengjing Hospital, China Medical University, and followed animal ethics and welfare regulations (Permission number: 2021PS741K). After one week of adaptive feeding, 1×10^7 Ishikawa cells transfected with inhibitor control, miR-329-3p inhibitor, and miR-329-3p inhibitor+*E2F1* shRNA were subcutaneously inoculated into the right flank of the mice. Tumor volume and body mass were measured every three days, with tumor volume calculated using the formula: volume = length × width ^ 2/2. Finally, on the 24th day, all mice were euthanized, and the tumors were photographed and harvested for subsequent H&E and IHC analysis.

Statistical analysis. All quantitative data were expressed as mean ± SD and statistical analyses were performed using GraphPad Prism 8.0. The differences between groups were analyzed using Student's t-test or one-way ANOVA. Pearson's correlation analysis was used to examine the correlation between *E2F1* level and clinicopathological features. Survival analysis for endometrial cancer patients and the diagnostic value of *E2F1* level were determined using the Kaplan-Meier method and receiver operating characteristic (ROC) curve, respectively. A p-value <0.05 was considered statistically significant.

Results

***E2F1* was ectopically overexpressed in EC and associated with poor prognosis.** To elucidate the expression pattern of *E2F1* in EC, we conducted IHC analysis on a training cohort consisting of 17 simple hyperplasia tissues, 22 atypical hyperplasia tissues, and 40 endometrial carcinoma tissues. Our findings revealed significantly higher expression of *E2F1* in EC tissues compared to simple hyperplasia or atypical

hyperplasia tissues. While simple hyperplasia and atypical hyperplasia tissues exhibited negative or weak *E2F1* expression, extensive *E2F1* staining was observed in EC tissues (Figure 1A). To further validate this observation, we assessed *E2F1* protein levels in three randomly selected samples from each group (simple hyperplasia, atypical hyperplasia, and EC) using qRT-PCR and western blotting. Consistent with our expectations, all EC specimens displayed higher levels of *E2F1* compared to the other two groups (Figures 1B, 1C). We categorized EC patients into two groups based on their IHC scores: high *E2F1* expression (60.0%, 24/40) and low *E2F1* expression (40%, 16/40), and proceeded to evaluate the correlation between *E2F1* level and clinicopathological characteristics. Table 2 illustrates the positive correlation between high *E2F1* expression and vascular space infiltration ($p<0.0001$), advanced FIGO stage ($p<0.004$), lymph node metastasis ($p=0.005$), depth of muscle infiltration ($p=0.002$), p53 mutation ($p=0.004$), and pathological types ($p=0.013$). Additionally, patients with poorly differentiated EC exhibited significantly higher *E2F1* expression compared to moderately or well-differentiated patients (Table 2).

Subsequently, we validated the expression pattern of *E2F1* in a large cohort from TCGA database and analyzed its association with clinicopathological characteristics. Once again, patients with high *E2F1* expression displayed advanced FIGO stage (Figure 1D). Furthermore, *E2F1* expression was associated with pathological types, with higher levels observed in serous carcinoma compared to endometrioid or mixed carcinoma ($p<0.0001$, Figure 1E). Importantly, Kaplan-Meier analysis demonstrated a significant correlation between higher *E2F1* expression and poorer overall survival in EC patients (hazard ratio [HR], 2.468; 95% CI, 1.58–3.81, $p<0.001$, Figure 1F). Additionally, the diagnostic value of *E2F1* for EC was assessed using ROC curves, yielding an area under the curve (AUC) of 0.952 (95% CI, 0.918–0.988, Figure 1G). Collectively, these findings suggest that *E2F1* may play an oncogenic role in the carcinogenesis and progression of EC and has the potential as a diagnostic marker for distinguishing EC patients from non-cancer individuals.

***E2F1* high expression facilitates tumorigenic properties of EC cells.** Motivated by the correlation between *E2F1* levels and histological grade, we investigated the expression levels of *E2F1* mRNA and proteins in three EC cell lines with varying degrees of differentiation. As anticipated, Ishikawa cells, representing well-differentiated cells, exhibited the lowest expression of *E2F1*, whereas KLE cells, characterized by poor differentiation, displayed the highest expression level among the three cell lines (Figures 2A, 2B). This observation suggests that *E2F1* holds promise as a potential biomarker for distinguishing tumor cell differentiation.

Subsequently, we explored whether cells with different *E2F1* levels exhibited distinct biological behaviors. We evaluated cell viability and cell cycle distribution of Ishikawa, HEC-1A, and KLE cells using the CCK-8 assay and flow cytometry, respectively. As illustrated in Figure 2C, there was a significant difference in cell viability among the three cell lines at 72 h and 96 h, while no significant difference was observed at 24 h and 48 h. KLE cells, characterized by high *E2F1* expression, demonstrated the strongest proliferative ability, whereas Ishikawa and HEC-1A cells displayed relatively weaker proliferative capacity. Similarly, flow cytometry analysis revealed that KLE cells exhibited rapid cell cycle progression, as evidenced by a decreased proportion of cells in the G1 phase and an increased population in the S phase. Conversely, cells with low *E2F1* levels (Ishikawa and HEC-1A) exhibited cell cycle arrest at the G1 phase and a blocked G1/S transition compared to KLE cells (Figures 2D, 2E).

Given the role of *E2F1* in promoting tumor cell metastasis through the regulation of target gene transcription, we investigated whether *E2F1* influenced the cell migration ability of endometrial carcinoma cells. As depicted in Figures 2F and 2G, the scratch healing rate of KLE cells was significantly higher than that of Ishikawa and HEC-1A cells, indicating a gradual improvement in cell migration ability with increased *E2F1* expression. Epithelial-mesenchymal transition (EMT) is a program initially recognized as essential during embryonic development and has later

Table 2. Correlation between *E2F1* level and clinicopathological characteristics of EC patients.

Clinicopathological features	Cases	E2F1 level (case)		p-value
		Low (n=16)	High (n=24)	
Age				0.685
>55	26	11	15	
≤55	14	5	9	
Vascular space invasion				< 0.001
Presence	13	0	13	
Absence	27	16	11	
FIGO stage				0.004
I	24	14	10	
II–IV	16	2	14	
Lymph node metastasis				0.005
Presence	9	0	9	
Absence	31	16	15	
Depth of muscle invasion				0.002
<1/2	23	14	9	
≥1/2	17	2	15	
p53 mutant				0.004
Presence	13	1	12	
Absence	27	15	12	
Pathological types				0.013
Adenocarcinoma	27	15	12	
Serous carcinoma	7	0	7	
Mixed carcinoma or other	6	1	5	
Differentiation status				0.0004
Poorly	13	1	12	
Moderately or well	27	15	12	

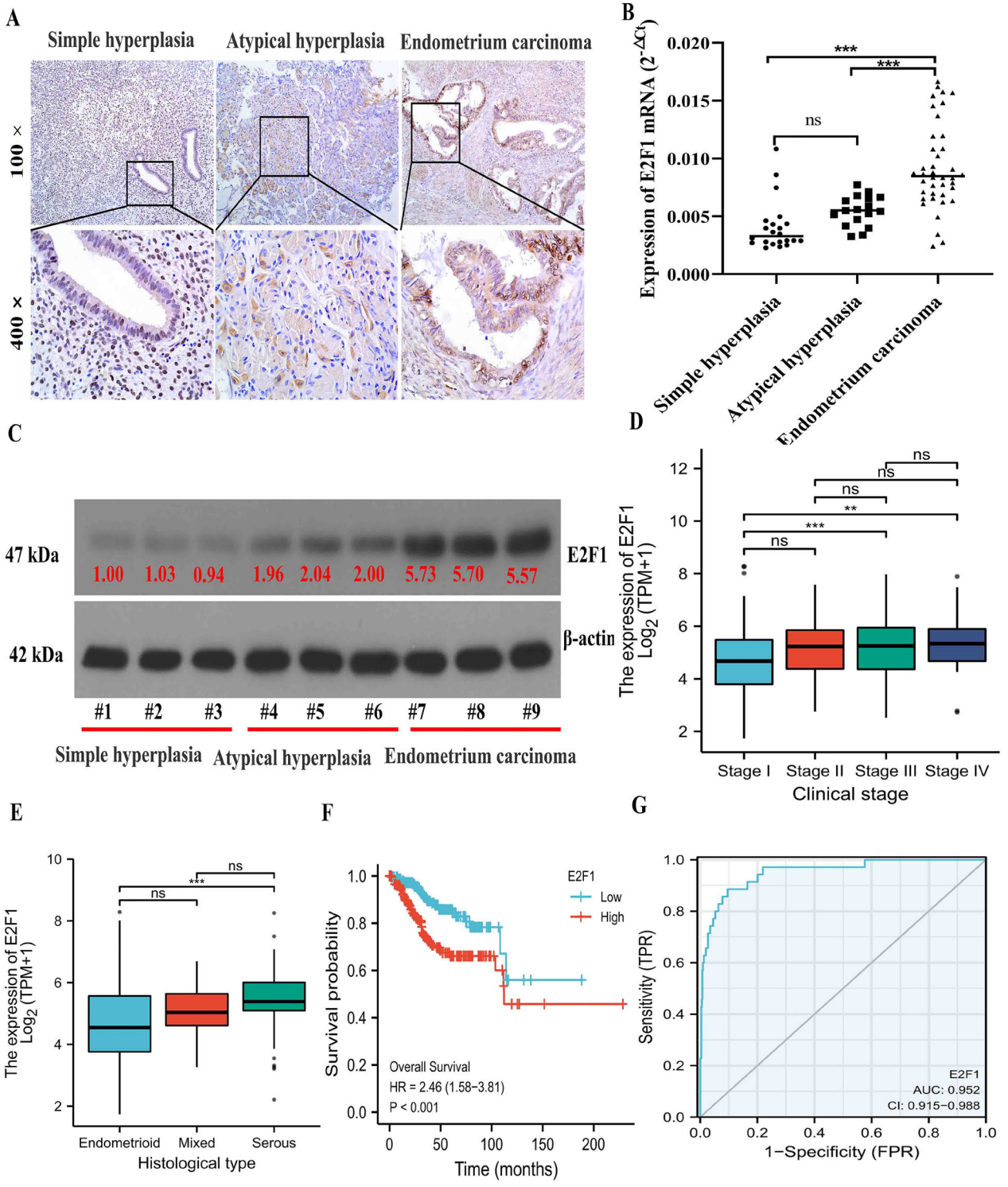

Figure 1. ***E2F1*** **was significantly increased in EC tissues and positively correlated with poor prognosis. A) Representative images of IHC staining of** ***E2F1*** **in simple hyperplasia tissues, atypical hyperplasia tissues, and EC tissues, magnification, 100× (up) and 400× (down). B) qRT-PCR analysis of** ***E2F1*** **mRNA expression level in simple hyperplasia (n = 17), atypical hyperplasia (n = 22), and EC (n = 40). C) Western blotting analysis of** ***E2F1*** **protein expression level in three randomly simple hyperplasia tissues, atypical hyperplasia tissues, and EC tissues. D)** ***E2F1*** **expression in EC tissues with different FIGO stage (stage I-IV). E)** ***E2F1*** **expression in endometrial carcinoma tissues with different histological types (endometrioid carcinoma, mixed carcinoma, and serous carcinoma). F) Overall survival curve of EC patients with high or low** ***E2F1*** **expression levels. G) ROC curves analysis of the accuracy of** ***E2F1*** **level for endometrial carcinoma diagnosis. **p<0.01, ***p<0.001 Abbreviations: HR-Hazard Ratio; AUC-area under curve; CI-confidence intervals; ns-no significance**

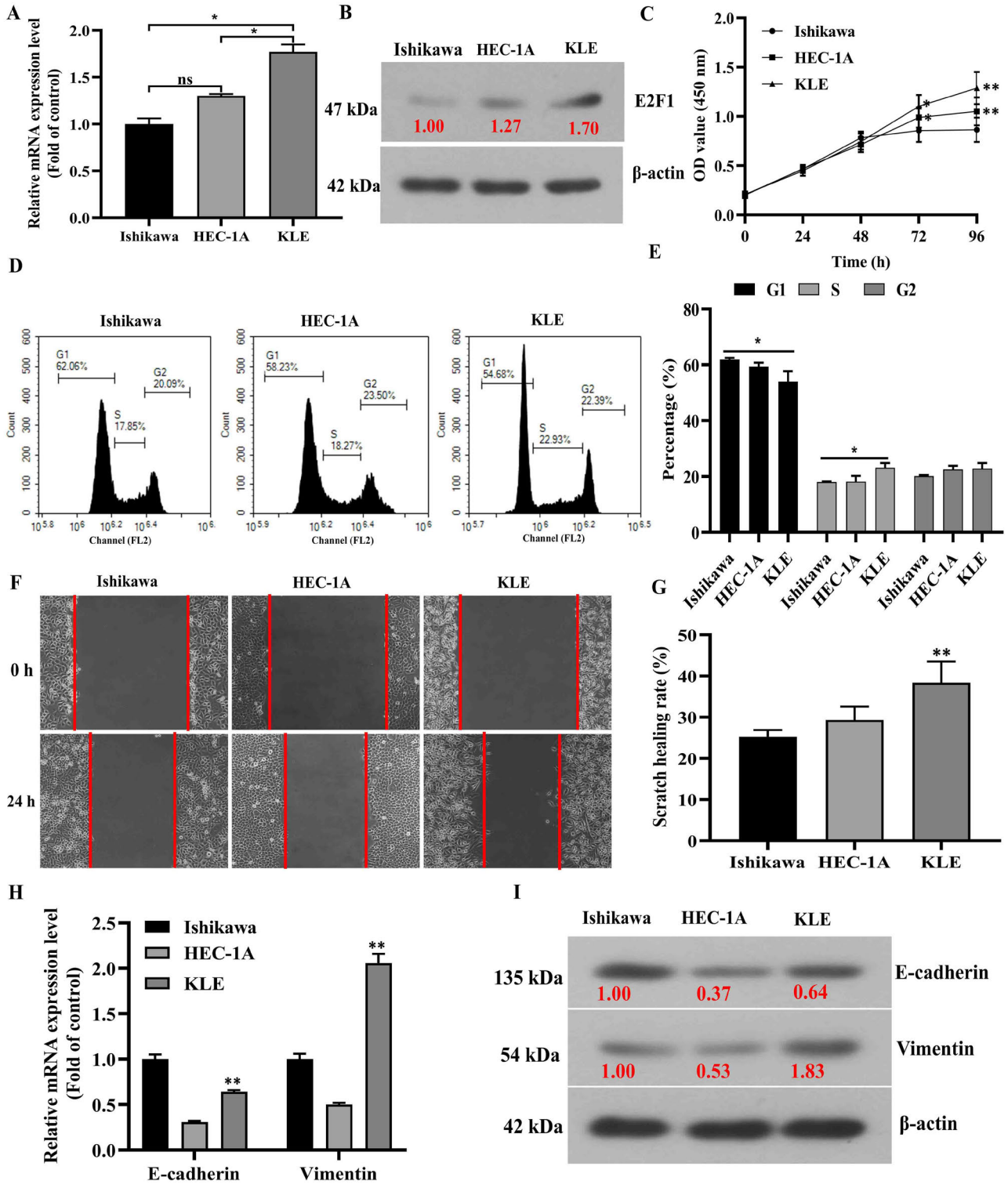

Figure 2. High *E2F1* expression was associated with poorly differentiated and promoted cell proliferation and the EMT process. A, B) qRT-PCR and western blotting analysis of *E2F1* mRNA and protein expression level in EC cells with different differentiation degrees (Ishikawa: well differentiated, HEC-1A: moderately differentiated, and KLE: poorly differentiated), respectively. C) CCK-8 analysis of the cell viability of Ishikawa, HEC-1A, and KLE cells after incubation for different times. D, E) Flow cytometry analysis of the cell cycle distribution of Ishikawa, HEC-1A, and KLE cells. F, G) Scratch healing assay analysis cell migration of Ishikawa, HEC-1A, and KLE cells. H, I) qRT-PCR and western blotting analysis of mRNA and protein levels of EMT-related markers (E-cadherin and Vimentin) in Ishikawa, HEC-1A, and KLE cells, respectively. *p<0.05, **p<0.01, ***p<0.001 Abbreviation: ns-no significance

been found to confer cell migration and invasion capabilities [26]. Therefore, we assessed the mRNA and protein expression levels of the epithelial marker E-cadherin and the mesenchymal marker Vimentin in the cells. Both qRT-PCR and western blotting analyses confirmed that KLE cells exhibited an increased level of Vimentin and a decreased level of E-cadherin, while Ishikawa cells showed the opposite trend (Figures 2H, 2I). Collectively, these findings suggest that *E2F1* may facilitate the tumorigenic properties of EC cells.

Silencing *E2F1* suppresses EC cell growth and metastasis. To further investigate the biological functions of *E2F1* in EC cells, we selected Ishikawa cells (with the lowest *E2F1* level) and KLE cells (with the highest *E2F1* level) as cell models for subsequent experiments. Initially, we transfected KLE cells and Ishikawa cells with *E2F1* siRNA and an overexpression plasmid (*E2F1* vector) to manipulate *E2F1* gene expression. The efficacy of *E2F1* silencing and overexpression was confirmed using qRT-PCR and western blotting analysis (Figures 3A, 3B).

As illustrated in Figures 3C–3F, overexpressing *E2F1* significantly enhanced cell proliferation, cell cycle progression, migration, and invasion of Ishikawa cells. Conversely, silencing *E2F1* in KLE cells markedly impaired these biological behaviors compared to the control group. Similarly, qRT-PCR and western blotting analysis demonstrated that *E2F1* knockdown upregulated E-cadherin and downregulated Vimentin, MMP2, and MMP9 in Ishikawa cells, while *E2F1* overexpression exhibited the opposite pattern in KLE cells (Figures 3G–3J).

Taken together, these findings suggest that *E2F1* plays a crucial role in the malignant proliferation and metastasis of EC cells.

***E2F1* serves as a potential target of miR-329-3p in endometrial carcinoma.** Despite demonstrating that *E2F1* acts as an oncogenic gene and enhances the tumorigenic properties of EC cells, its underlying mechanism remains largely unknown. Given the significant roles of miRNAs in tumorigenesis and cancer progression [21, 27, 28], we utilized the Target Scan (http://www.targetscan.org/) and starBase (http://starbase.sysu.edu.cn/) databases to identify putative miRNAs capable of binding to the *E2F1* 3'UTR. Among these predicted miRNAs, miR-329-3p was chosen due to its tumor suppressor role and high-scoring miRNA-target interactions. Figure 4A illustrates the potential complementary sites for miR-329-3p within the *E2F1* 3'UTR region (position 200–207). Furthermore, we confirmed the targeting relationship between miR-329-3p and *E2F1* through a luciferase reporter assay. As expected, co-transfection of miR-329-3p mimics with the wild-type *E2F1*-3'UTR led to a significant reduction in luciferase activity, while no discernible change was observed in cells co-transfected with miR-329-3p mimics and mutant *E2F1*-3'UTR (Figure 4B), indicating that *E2F1* is targeted by miR-329-3p.

Next, we investigated the expression level of miR-329-3p in clinical samples and cell lines using qRT-PCR analysis. Consistently, our results demonstrated a significant downregulation of miR-329-3p in EC tissues compared to hyperplasia or atypical hyperplasia tissues (Figure 4C). Moreover, miR-329-3p exhibited an inverse expression pattern with *E2F1*, as evidenced by the low *E2F1* expression in tumor tissues or cells exhibiting high miR-329-3p levels. Western blotting and qRT-PCR analysis further confirmed that miR-329-3p inhibitor increased *E2F1* expression at both the mRNA and protein levels, whereas miR-329-3p mimics reduced *E2F1* expression compared to the control group (Figures 4E–4G). Collectively, these results indicate that miR-329-3p directly targets *E2F1* and negatively regulates its expression.

Subsequently, we evaluated whether miR-329-3p mimics could rescue the tumor-promoting effect of *E2F1* in EC cells. Rescue experiments were conducted using miR-329-3p inhibitor and mimics after depleting *E2F1* (*E2F1* siRNA) or inducing its overexpression (*E2F1*-vector) (Figures 4E–4G). As anticipated, transfection of miR-329-3p inhibitor significantly enhanced cell proliferation, cell cycle progression, migration, invasion, and the EMT process in Ishikawa cells. However, silencing *E2F1* effectively abolished this promoting effect. Similarly, transfection of miR-329-3p mimics significantly inhibited cell proliferation, cell cycle progression, migration, invasion, and the EMT process in KLE cells, while *E2F1* overexpression rescued the repressive effect of miR-329-3p (Figures 5A–5I). Collectively, these findings confirm that miR-329-3p can suppress the proliferation and metastasis of EC cells by directly and negatively regulating *E2F1* expression.

miR-329-3p inhibits EC growth and metastasis through targeting *E2F1*. To further confirm whether miR-329-3p suppresses tumorigenesis and progression of EC by downregulating *E2F1*, we established a xenograft nude model using subcutaneous inoculation of Ishikawa cells stably transfected with inhibitor-control, miR-329-3p inhibitor, and miR-329-3p inhibitor+*E2F1* shRNA. The results showed that tumors in the miR-329-3p inhibitor group had significantly larger volume and higher weight compared to the control group. However, *E2F1* silencing partially mitigated the tumor-promoting effect caused by miR-329-3p antagomir (Figures 6A–6C). Moreover, H&E staining of tumor slices revealed conspicuous necrosis in the miR-329-3p inhibitor+*E2F1* shRNA group compared to the miR-329-3p inhibitor group (Figure 6D), indicating significant cell apoptosis in the tissues. Additionally, IHC results demonstrated that tumor tissues in the miR-329-3p inhibitor group exhibited higher expression of Ki-67, *E2F1*, Vimentin, MMP2, MMP9, and lower expression of E-cadherin compared to the control group, with these effects being partially rescued by *E2F1* silencing (Figures 6E, 6F). In summary, these findings suggest that miR-329-3p inhibits the oncogenesis of EC cells *in vivo*, at least partially, by suppressing *E2F1* levels.

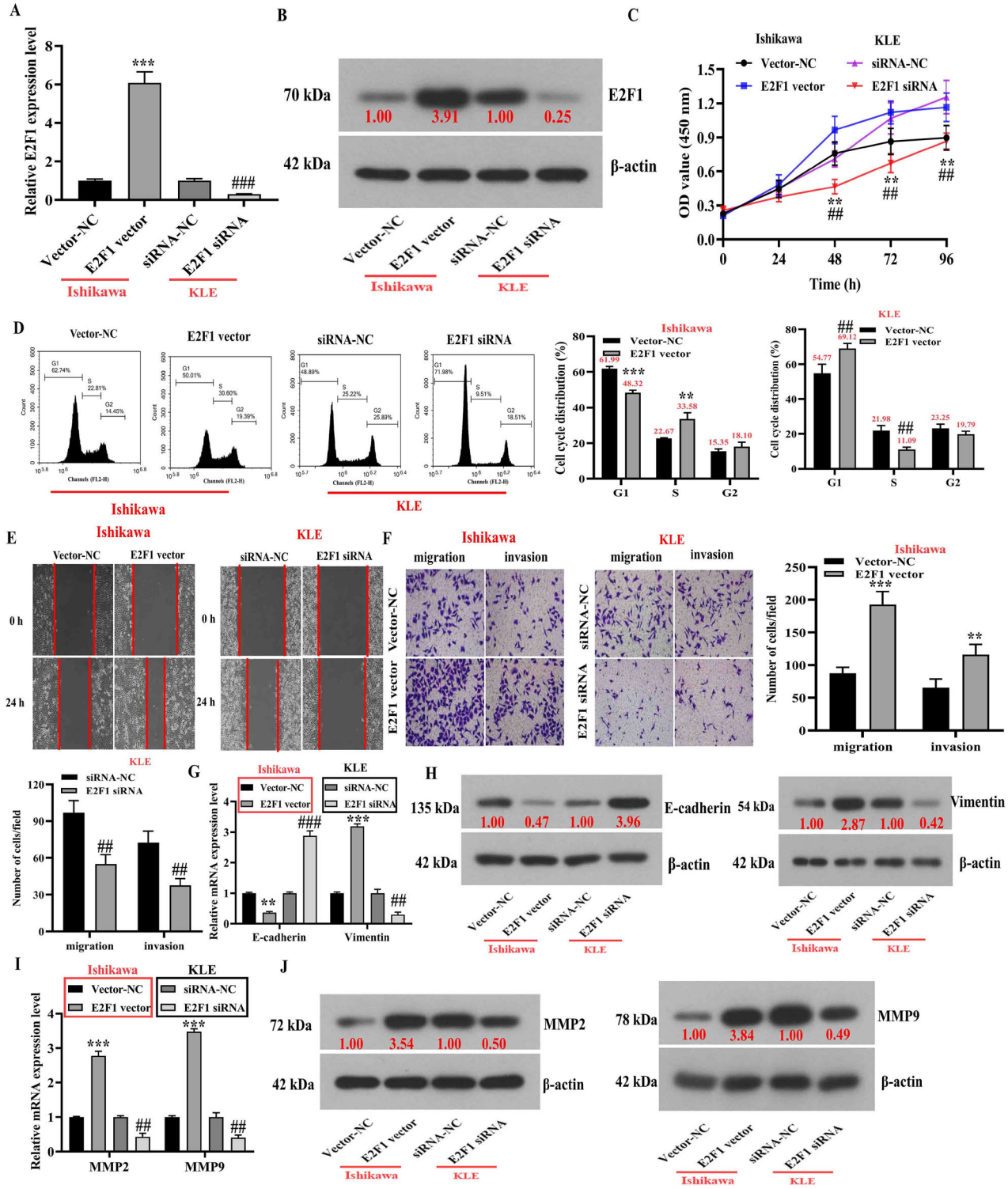

Figure 3. ***E2F1*** **overexpression facilitates cell proliferation, cell cycle, migration, and invasion of EC cells. A, B) Ishikawa and KLE cells were transfected with** ***E2F1*** **vector and** ***E2F1*** **si-RNAs for 48 h, qRT-PCR and western blotting analysis of the transfection efficiency, respectively. C) CCK-8 assay analysis of the cell viability of Ishikawa and KLE cells after transfection with** ***E2F1*** **vector or** ***E2F1*** **si-RNA. D) Flow cytometry analysis of the cell cycle distribution of Ishikawa and KLE cells. E, F) Scratch healing assay, Transwell migration, and Transwell invasion assay analysis of cell migration and invasion abilities in Ishikawa and KLE cells. G-J) qRT-PCR and western blotting analysis of mRNA and protein levels of E-cadherin, Vimentin, MMP2, and MMP9 in** ***E2F1*****-vector transfected Ishikawa cells and** ***E2F1*** **si-RNA transfected KLE cells, respectively., **p<0.01, ***p<0.001 compared with vector-NC group; ##p<0.01, ###p<0.001 compared with siRNA-NC group**

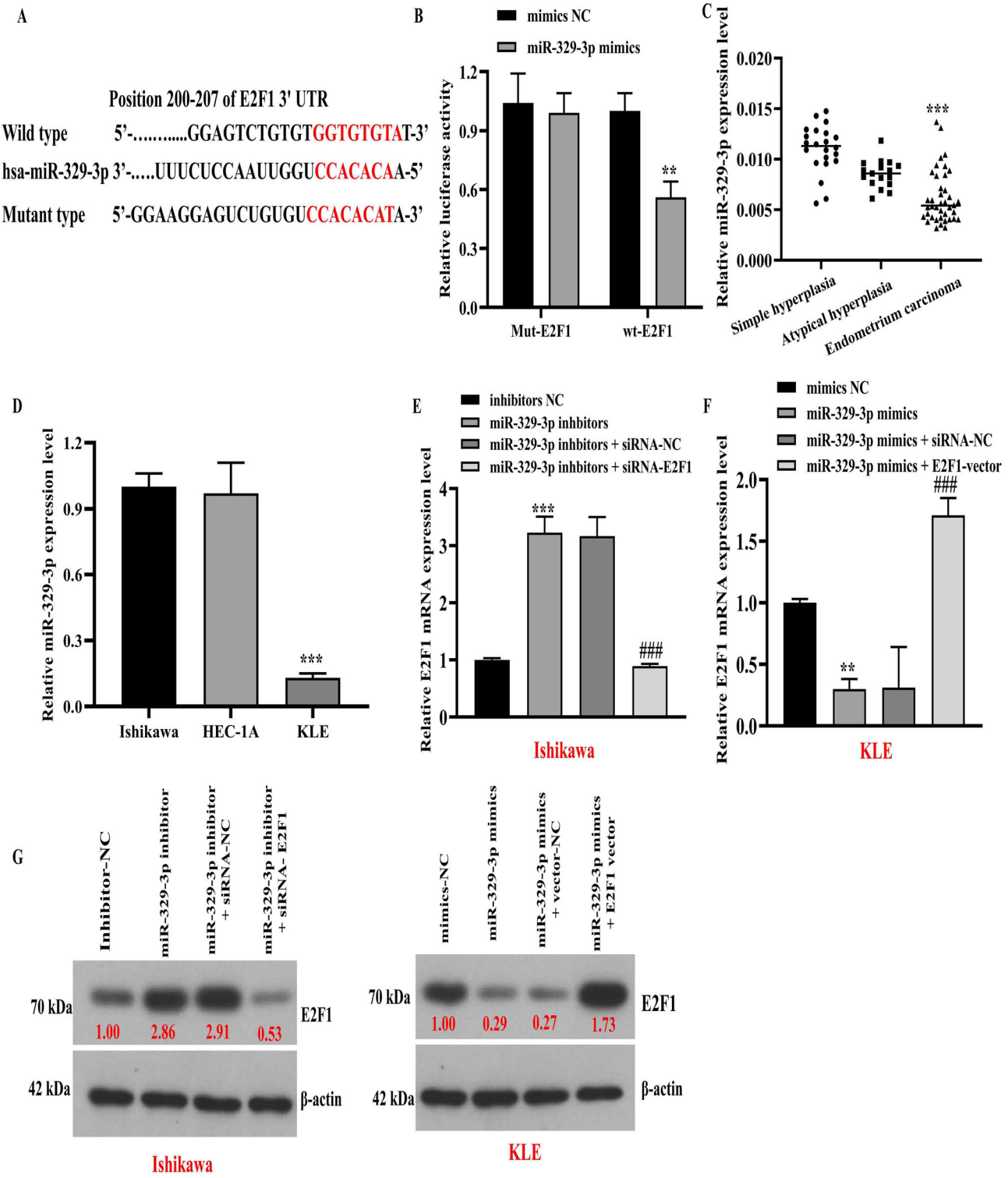

Figure 4. ***E2F1*** **is a target gene of miR-329-3p. A) Bioinformatics tools prediction of the potential binding site of miR-329-3p in 3' UTR of** ***E2F1*****. B) Dual-luciferase reporter gene assay validation of the targeting relationship between** ***E2F1*** **and miR-329-3p. C) qRT-PCR analysis of miR-329-3p expression in simple hyperplasia, atypical hyperplasia, and EC tissues. D) qRT-PCR analysis of miR-329-3p level in EC cells with different differentiation degrees (Ishikawa: well differentiated, HEC-1A: moderately differentiated, and KLE: poorly differentiated). E-G) Ishikawa cells were transfected with miR-329-3p inhibitor alone or co-transfected with** ***E2F1*** **si-RNA, while KLE cells were transfected with miR-329-3p mimics alone or co-transfected with** ***E2F1*** **vector for 48 h, qRT-PCR and western blotting analysis of** ***E2F1*** **mRNA and protein level in cells., **p<0.01, ***p<0.001 compared with mimics-NC group; ###p<0.001 compared with miR-329-3p mimics+siRNA group**

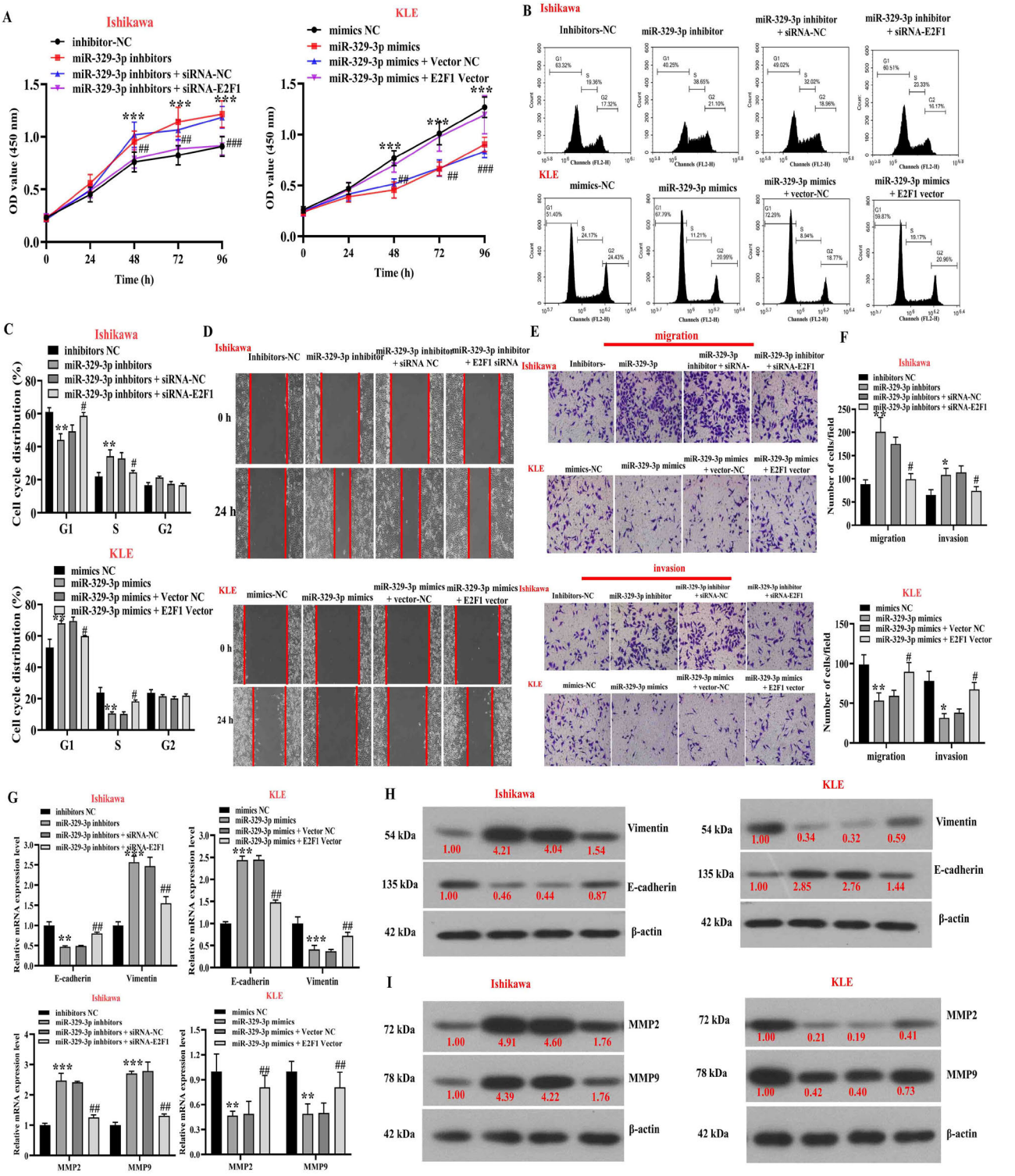

Figure 5. miR-329-3p overexpression effectively rescues *E2F1*-induced malignant biology behavior of EC cells. Ishikawa cells were transfected with miR-329-3p inhibitor alone or co-transfected with *E2F1* si-RNA, while KLE cells were transfected with miR-329-3p mimics alone or co-transfected with *E2F1* vector for 48 h. A-C) Cell proliferation and cell cycle distribution in cells were evaluated using CCK-8 assay and flow cytometry assay, respectively. D-F) Cell migration and invasion were determined using scratch healing assay, Transwell migration, and Transwell invasion assays, respectively. G-I) mRNA and protein expression levels of E-cadherin, Vimentin, MMP-2, and MMP-9 in cells were examined using qRT-PCR and western blotting, respectively. In Ishikawa cells: **p<0.01, ***p<0.001 compared with miR-329-3p inhibitor group; #p<0.05, ##p<0.01, ###p<0.001 compared with miR-329-3p inhibitor+siRNA-NC group. In KLE cells: **p<0.01, ***p<0.001 compared with miR-329-3p mimics group; #p<0.05, ##p<0.01, ###p<0.001 compared with miR-329-3p mimics+Vector-NC group

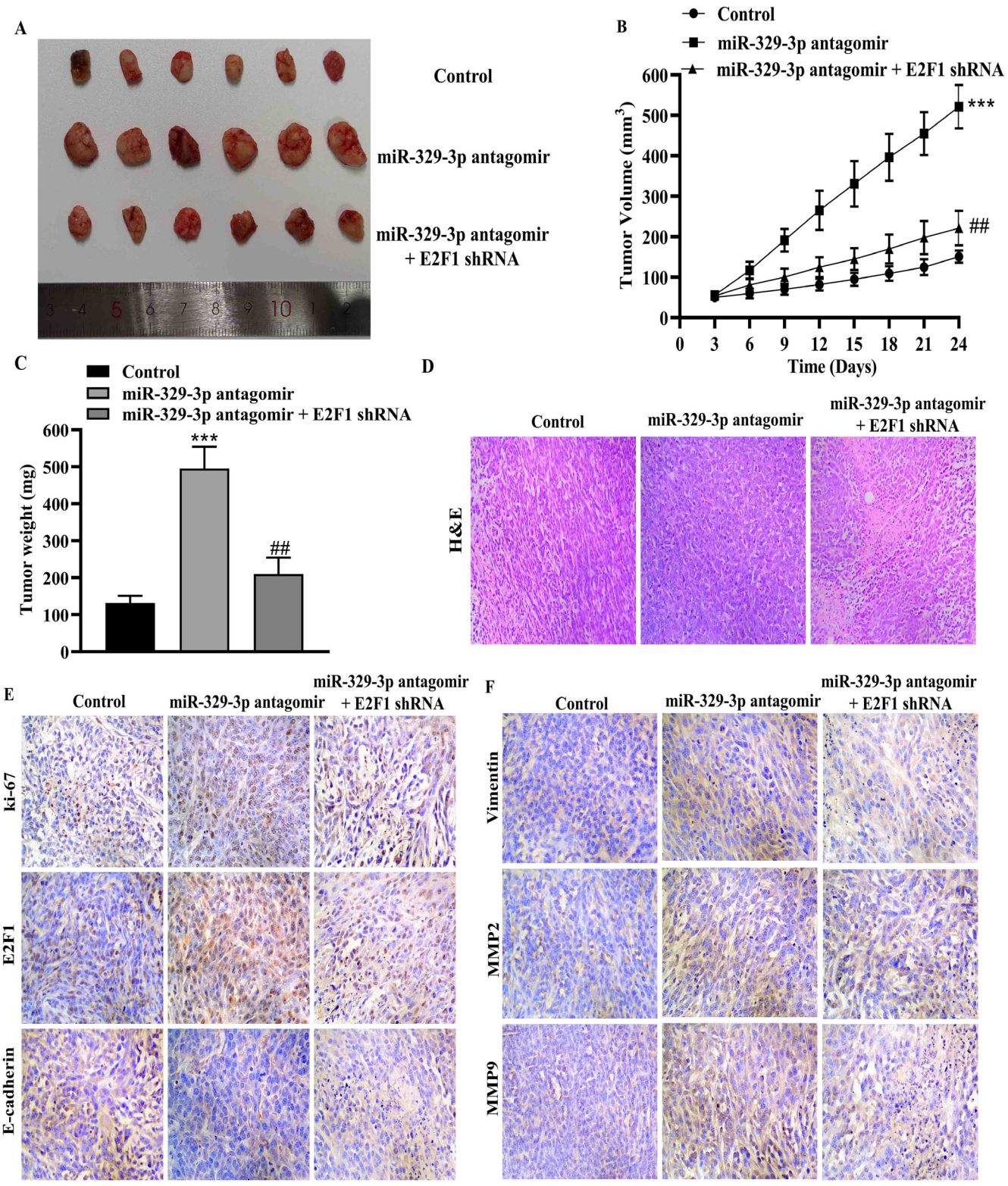

Figure 6. miR-329-3p suppresses tumor growth and metastasis through downregulating *E2F1*. A, B) Representative pictures of dissected tumors from tumor-bearing mice. B) Tumor growth curve. C) Tumor weight. D) H&E analysis of the pathological changes in tumor tissues from various groups. E, F) IHC analysis of the expression of Ki-67, *E2F1*, E-cadherin, Vimentin, MMP2, and MMP9 in tumor sections. Magnification: 400×

Discussion

EC, the most frequent gynecologic malignancy in North America and Western Europe, is attributed to the increasing prevalence of obesity or obesity-related metabolic syndrome [29]. Despite advancements in understanding EC's genetic diversity and epigenetic changes, its incidence and associated mortality continue to rise [30]. Therefore, it is crucial to mine predictive biomarkers, elucidate the pathogenesis and molecular mechanisms of EC, and improve patient prognosis. In this study, we observed a significant increase in *E2F1* expression in EC tumor tissues, which is closely correlated with poor patient prognosis. Mechanistically, we identified *E2F1* as a downstream target gene of miR-329-3p, which binds to the 3'UTR region of *E2F1*, resulting in its downregulation.

The transcription factor *E2F1* plays a pivotal role in mediating multiple cancer hallmark capabilities, including cell cycle regulation, survival, apoptosis, metabolism, and metastasis. Aberrant activation of *E2F1* is closely associated with poor clinical outcomes in various human cancers [31, 32]. Consistent with published literature, our results confirmed that *E2F1* overexpression significantly promotes cell proliferation, cell cycle progression, and metastasis of EC cells, highlighting its oncogenic role in EC. Interestingly, while numerous studies have validated the oncogenic role of *E2F1* in promoting carcinogenesis and progression, conflicting results have been reported regarding its tumor suppressor role, particularly in prostate cancer [14]. Additionally, conflicting roles of *E2F1* have been observed in response to anti-cancer therapies. For example, Knudsen et al. [33] demonstrated that depleting RB and activating *E2F1* effectively enhances the chemosensitivity of cisplatin, anti-microtubule agents, and topoisomerase inhibitors against prostate cancer cells. Moreover, *E2F1* overexpression potentiates the pro-apoptotic efficacy of etoposide in LNCaP cells [34]. Furthermore, ectopic expression of *E2F1* increases radiosensitivity in xenografted LNCaP and PC3 cells [35, 36]. These conflicting roles of *E2F1* also extend to its effect on cell apoptosis. On one hand, *E2F1* can block the degradation of p53 by activating p14/p19, subsequently inhibiting cell cycle progression and inducing apoptosis. *E2F1* can also trigger cell apoptosis by regulating p73, CASP-3, CASP-7, and TRAF2 expression [37]. On the other hand, numerous studies have confirmed that *E2F1* activation confers tumor cells with the ability to escape apoptotic cell death and facilitates tumorigenesis [13]. Collectively, these data underscore the critical role of *E2F1* in EC proliferation and metastasis, suggesting that targeting *E2F1* may hold promise as a therapeutic strategy for EC patients.

With an increasing understanding of miRNA's biological functions in development and disease, miRNAs have become attractive tools and targets for tumor diagnosis and treatment [38]. Existing studies have shown that miRNAs can exhibit both tumor-promoting and tumor-suppressing effects in tumorigenesis and progression [39]. Importantly, multiple miRNAs have demonstrated potential applications in tumor classification, diagnosis, targeted therapy, and prognosis evaluation [40, 41]. Since miRNAs mainly participate in tumor occurrence and development by regulating downstream target genes, we identified putative miRNAs that bind to the *E2F1* 3'UTR using bioinformatics databases. We demonstrated that miR-329-3p directly binds to *E2F1*, leading to its downregulation in EC cells. Furthermore, miR-329-3p was significantly downregulated in EC tissues and cells, and miR-329-3p mimics effectively rescued the malignant phenotype induced by *E2F1* overexpression *in vitro* and *in vivo*. Our findings highlight miR-329-3p as a tumor suppressor miRNA that reduces EC tumor growth and metastasis by downregulating the oncogenic gene *E2F1*. It is worth noting that miRNAs can target multiple downstream genes, and the same gene can also be regulated by multiple miRNAs [42]. Several studies have confirmed that multiple miRNAs directly regulate *E2F1* and affect tumor progression, including miR-25 [43], miR-20b [44], and miR-205-5p [45]. In our study, we demonstrate that miR-329-3p overexpression suppresses EC cell proliferation, cell cycle progression, metastasis, and the EMT phenotype. Consistently, several studies have validated the tumor suppressor role of miR-329-3p in various malignant tumors, including hepatocellular carcinoma [46], cervical cancer [47], and colorectal cancer [48].

The current study concludes that *E2F1* plays an oncogenic role in the progression of EC by regulating cell proliferation, cell cycle progression, migration, invasion, and the EMT process. Moreover, mechanistic studies demonstrated the direct binding of miR-329-3p to the 3'UTR region of *E2F1* mRNA, resulting in the downregulation of its expression. Collectively, these findings establish a theoretical foundation for the miR-329-3p/*E2F1* axis in the pathogenesis of EC.

References

[1] AMANT F, MOERMAN P, NEVEN P, TIMMERMAN D, VAN LIMBERGEN E et al. Endometrial cancer. Lancet 2005; 366: 491–505. https://doi.org/10.1016/s0140-6736(05)67063-8

[2] MAKKER V, MACKAY H, RAY-COQUARD I, LEVINE DA, WESTIN SN et al. Endometrial cancer. Nature Rev Dis Primers 2021; 7: 88. https://doi.org/10.1038/s41572-021-00324-8

[3] BROOKS RA, FLEMING GF, LASTRA RR, LEE NK, MORONEY JW et al. Current recommendations and recent progress in endometrial cancer. CA Cancer J Clinics 2019; 69: 258–279. https://doi.org/10.3322/caac.21561

[4] CROSBIE EJ, KITSON SJ, MCALPINE JN, MUKHOPADHYAY A, POWELL ME et al. Endometrial cancer. Lancet 2022; 399: 1412–1428. https://doi.org/10.1016/s0140-6736(22)00323-3

[5] LAMMENS T, LI J, LEONE G, DE VEYLDER L. Atypical E2Fs: new players in the E2F transcription factor family. Trends Cell Biol 2009; 19: 111–118. https://doi.org/10.1016/j.tcb.2009.01.002

[6] WEIJTS B, WESTENDORP B, HIEN BT, MARTÍNEZ-LÓPEZ LM, ZIJP M et al. Atypical E2Fs inhibit tumor angiogenesis. Oncogene 2018; 37: 271–276. https://doi.org/10.1038/onc.2017.336

[7] JUSINO S, SAAVEDRA HI. Role of E2Fs and mitotic regulators controlled by E2Fs in the epithelial to mesenchymal transition. Exp Biol Med 2019; 244: 1419–1429. https://doi.org/10.1177/1535370219881360

[8] MANDIGO AC, YUAN W, XU K, GALLAGHER P, PANG A et al. RB/E2F1 as a Master Regulator of Cancer Cell Metabolism in Advanced Disease. Cancer Dis 2021; 11: 2334–2353. https://doi.org/10.1158/2159-8290.cd-20-1114

[9] ZHU Q, ZHANG C, QU T, LU X, HE X et al. MNX1-AS1 Promotes Phase Separation of IGF2BP1 to Drive c-Myc-Mediated Cell-Cycle Progression and Proliferation in Lung Cancer. Cancer Res 2022; 82: 4340–4358. https://doi.org/10.1158/0008-5472.can-22-1289

[10] RODRIGUEZ-BRAVO V, PIPPA R, SONG WM, CARCELES-CORDON M, DOMINGUEZ-ANDRES A et al. Nuclear Pores Promote Lethal Prostate Cancer by Increasing POM121-Driven E2F1, MYC, and AR Nuclear Import. Cell 2018; 174: 1200–1215.e20. https://doi.org/10.1016/j.cell.2018.07.015

[11] ZHENG X, HUANG M, XING L, YANG R, WANG X et al. The circRNA circSEPT9 mediated by E2F1 and EIF4A3 facilitates the carcinogenesis and development of triple-negative breast cancer. Mol Cancer 2020; 19: 73. https://doi.org/10.1186/s12943-020-01183-9

[12] JING Z, LIU Q, HE X, JIA Z, XU Z et al. NCAPD3 enhances Warburg effect through c-myc and E2F1 and promotes the occurrence and progression of colorectal cancer. J Exp Clin Cancer Res 2022; 41: 198. https://doi.org/10.1186/s13046-022-02412-3

[13] LIN X, HAN T, XIA Q, CUI J, ZHUO M et al. CHPF promotes gastric cancer tumorigenesis through the activation of E2F1. Cell Death Dis 2021; 12: 876. https://doi.org/10.1038/s41419-021-04148-y

[14] CHUN JN, CHO M, PARK S, SO I, JEON JH. The conflicting role of E2F1 in prostate cancer: A matter of cell context or interpretational flexibility? Biochim Biophys Acta Rev Cancer 2020; 1873: 188336. https://doi.org/10.1016/j.bbcan.2019.188336

[15] XU Q, GE Q, ZHOU Y, YANG B, YANG Q et al. MELK promotes Endometrial carcinoma progression via activating mTOR signaling pathway. EBioMedicine 2020; 51: 102609. https://doi.org/10.1016/j.ebiom.2019.102609

[16] ZHANG Y, WANG Z, MA J, HUO J, LI Y et al. Bioinformatics Identification of the Expression and Clinical Significance of E2F Family in Endometrial Cancer. Front Genetics 2020; 11: 557188. https://doi.org/10.3389/fgene.2020.557188

[17] YANG X, CHENG Y, LI X, ZHOU J, DONG Y et al. A Novel Transcription Factor-Based Prognostic Signature in Endometrial Cancer: Establishment and Validation. Onco Targets Ther 2021; 14: 2579–2598. https://doi.org/10.2147/ott.s293085

[18] LU TX, ROTHENBERG ME. MicroRNA. J Allergy Clin Immunol 2018; 141: 1202–1207. https://doi.org/10.1016/j.jaci.2017.08.034

[19] MORI MA, LUDWIG RG, GARCIA-MARTIN R, BRANDÃO BB, KAHN CR. Extracellular miRNAs: From Biomarkers to Mediators of Physiology and Disease. Cell Metab 2019; 30: 656–673. https://doi.org/10.1016/j.cmet.2019.07.011

[20] KABEKKODU SP, SHUKLA V, VARGHESE VK, D' SOUZA J, CHAKRABARTY S et al. Clustered miRNAs and their role in biological functions and diseases. Biol Rev Camb Philos Soc 2018; 93: 1955–1986. https://doi.org/10.1111/brv.12428

[21] HE B, ZHAO Z, CAI Q, ZHANG Y, ZHANG P et al. miRNA-based biomarkers, therapies, and resistance in Cancer. Int J Biol Sci 2020; 16: 2628–2647. https://doi.org/10.7150/ijbs.47203

[22] GJORGJIEVA M, SOBOLEWSKI C, DOLICKA D, CORREIA DE SOUSA M, FOTI M. miRNAs and NAFLD: from pathophysiology to therapy. Gut 2019; 68: 2065–2079. https://doi.org/10.1136/gutjnl-2018-318146

[23] LIU X, ZHANG Y, WANG Y, BIAN C, WANG F. Long non-coding RNA KCNQ1OT1 up-regulates CTNND1 by sponging miR-329-3p to induce the proliferation, migration, invasion, and inhibit apoptosis of colorectal cancer cells. Cancer Cell Int 2020; 20: 340. https://doi.org/10.1186/s12935-020-01425-2

[24] GUO X, WANG Y. LncRNA TMPO-AS1 promotes hepatocellular carcinoma cell proliferation, migration and invasion through sponging miR-329-3p to stimulate FOXK1-mediated AKT/mTOR signaling pathway. Cancer Med 2020; 9: 5235–5246. https://doi.org/10.1002/cam4.3046

[25] LI G, LI Y, WANG DY. Overexpression of miR-329-3p sensitizes osteosarcoma cells to cisplatin through suppression of glucose metabolism by targeting LDHA. Cell Biol Int 2021; 45: 766–774. https://doi.org/10.1002/cbin.11476

[26] MITTAL V. Epithelial Mesenchymal Transition in Tumor Metastasis. Ann Rev Pathol 2018; 13: 395–412. https://doi.org/10.1146/annurev-pathol-020117-043854

[27] RUPAIMOOLE R, SLACK FJ. MicroRNA therapeutics: towards a new era for the management of cancer and other diseases. Nat Rev Drug Dis 2017; 16: 203–222. https://doi.org/10.1038/nrd.2016.246

[28] LEE YS, DUTTA A. MicroRNAs in cancer. Ann Rev Pathol 2009; 4: 199–227. https://doi.org/10.1146/annurev.pathol.4.110807.092222

[29] PASSARELLO K, KURIAN S, VILLANUEVA V. Endometrial Cancer: An Overview of Pathophysiology, Management, and Care. Semin Oncol Nurs 2019; 35: 157–165. https://doi.org/10.1016/j.soncn.2019.02.002

[30] LU KH, BROADDUS RR. Endometrial Cancer. N Engl J Med 2020; 383: 2053–2064. https://doi.org/10.1056/NEJMra1514010

[31] TIAN W, CUI F, ESTEBAN MA. E2F1 in renal cancer: Mr Hyde disguised as Dr Jekyll? The J Pathol 2013; 231: 143–146. https://doi.org/10.1002/path.4238

[32] EL DIKA M. Redirecting E2F1 to TA-p73 improves cancer therapy through apoptotic induction. DNA Repair 2020; 90: 102858. https://doi.org/10.1016/j.dnarep.2020.102858

[33] SHARMA A, COMSTOCK CE, KNUDSEN ES, CAO KH, HESS-WILSON JK et al. Retinoblastoma tumor suppressor status is a critical determinant of therapeutic response in prostate cancer cells. Cancer Res 2007; 67: 6192–6203. https://doi.org/10.1158/0008-5472.can-06-4424

[34] LIBERTINI SJ, TEPPER CG, GUADALUPE M, LU Y, ASMUTH DM et al. E2F1 expression in LNCaP prostate cancer cells deregulates androgen dependent growth, suppresses differentiation, and enhances apoptosis. Prostate 2006; 66: 70–81. https://doi.org/10.1002/pros.20314

[35] UDAYAKUMAR TS, HACHEM P, AHMED MM, AGRAWAL S, POLLACK A. Antisense MDM2 enhances E2F1-induced apoptosis and the combination sensitizes androgen-sensitive [corrected] and androgen-insensitive [corrected] prostate cancer cells to radiation. Mol Cancer res 2008; 6: 1742–1754. https://doi.org/10.1158/1541-7786.mcr-08-0102

[36] UDAYAKUMAR TS, STOYANOVA R, HACHEM P, AHMED MM, POLLACK A. Adenovirus E2F1 overexpression sensitizes LNCaP and PC3 prostate tumor cells to radiation in vivo. Int J Radiat Oncol Biol Phys 2011; 79: 549–558. https://doi.org/10.1016/j.ijrobp.2010.08.013

[37] BELL LA, RYAN KM. Life and death decisions by E2F-1. Cell Death Diff 2004; 11: 137–142. https://doi.org/10.1038/sj.cdd.4401324

[38] MAHTAL N, LENOIR O, TINEL C, ANGLICHEAU D, THARAUX PL. MicroRNAs in kidney injury and disease. Nat Rev Nephrol 2022; 18: 643–662. https://doi.org/10.1038/s41581-022-00608-6

[39] MENON A, ABD-AZIZ N, KHALID K, POH CL, NAIDU R. miRNA: A Promising Therapeutic Target in Cancer. Int J Mol Sci 2022; 23: 11502. https://doi.org/10.3390/ijms231911502

[40] KARA G, CALIN GA, OZPOLAT B. RNAi-based therapeutics and tumor targeted delivery in cancer. Adv Drug Del Rev 2022; 182: 114113. https://doi.org/10.1016/j.addr.2022.114113

[41] CHEN B, DRAGOMIR MP, YANG C, LI Q, HORST D et al. Targeting non-coding RNAs to overcome cancer therapy resistance. Signal Transduct Target Ther 2022; 7: 121. https://doi.org/10.1038/s41392-022-00975-3

[42] SILVESTRO S, GUGLIANDOLO A, CHIRICOSTA L, DI-OMEDE F, TRUBIANI O et al. MicroRNA Profiling of HL-1 Cardiac Cells-Derived Extracellular Vesicles. Cells 2021; 10: 273. https://doi.org/10.3390/cells10020273

[43] ZHAO Y, JIN LJ, ZHANG XY. Exosomal miRNA-205 promotes breast cancer chemoresistance and tumorigenesis through E2F1. Aging 2021; 13: 18498–18514. https://doi.org/10.18632/aging.203298

[44] LI SY, ZHU Y, LI RN, HUANG JH, YOU K et al. LncRNA Lnc-APUE is Repressed by HNF4α and Promotes G1/S Phase Transition and Tumor Growth by Regulating MiR-20b/E2F1 Axis. Adv Sci (Weinh) 2021; 8: 2003094. https://doi.org/10.1002/advs.202003094

[45] QIAN Q, MA Q, WANG B, QIAN Q, ZHAO C et al. MicroRNA-205-5p targets E2F1 to promote autophagy and inhibit pulmonary fibrosis in silicosis through impairing SKP2-mediated Beclin1 ubiquitination. J Cell Mol Med 2021; 25: 9214–9227. https://doi.org/10.1111/jcmm.16825

[46] XIN RQ, LI WB, HU ZW, WU ZX, SUN W. MiR-329-3p inhibits hepatocellular carcinoma cell proliferation and migration through USP22-Wnt/β-Catenin pathway. Eur Rev Med Pharmacol Sci 2020; 24: 9932–9939. https://doi.org/10.26355/eurrev_202010_23204

[47] XU J, ZHANG J. LncRNA TP73-AS1 is a novel regulator in cervical cancer via miR-329-3p/ARF1 axis. J Cell Biochem 2020; 121: 344–352. https://doi.org/10.1002/jcb.29181

[48] FANG X, XU Y, LI K, LIU P, ZHANG H et al. Exosomal lncRNA PCAT1 Promotes Tumor Circulating Cell-Mediated Colorectal Cancer Liver Metastasis by Regulating the Activity of the miR-329-3p/Netrin-1-CD146 Complex. J Immunol Res 2022; 2022: 9916228. https://doi.org/10.1155/2022/9916228